

Study of Self-Interaction Errors in Density-Functional Calculations of Magnetic Exchange Coupling Constants Using Three Self-Interaction-Correction Methods

Prakash Mishra,[†] Yoh Yamamoto,[‡] Po-Hao Chang,[‡] Duyen B. Nguyen,[¶] Juan E. Peralta,[¶] Tunna Baruah,^{†,‡} and Rajendra R. Zope^{*,†,‡}

[†]*Computational Science Program, University of Texas at El Paso, El Paso, Texas 79968, USA*

[‡]*Department of Physics, University of Texas at El Paso, El Paso, TX, 79968, USA*

[¶]*Physics Department and Science of Advanced Materials Program, Central Michigan University, Mt. Pleasant, Michigan 48859, USA*

E-mail: rzope@utep.edu

Abstract

We examine the role of self-interaction errors (SIE) removal on the evaluation of magnetic exchange coupling constants. In particular we analyze the effect of scaling down the self-interaction-correction (SIC) for three *non-empirical* density functional approximations (DFAs) namely, the local spin density approximation, the Perdew-Burke-Ernzerhof generalized gradient approximation, and recent SCAN family of meta-GGA functionals. To this end, we employ three one-electron SIC methods: Perdew-Zunger [Perdew, J. P.; Zunger, A. *Phys. Rev. B*, **1981**, *23*, 5048] SIC, the orbitalwise scaled SIC method [Vydrov, O. A. *et al.*, *J. Chem. Phys.* **2006**, *124*, 094108], and the

recent local scaling method [Zope, R. R. *et al.*, *J. Chem. Phys.* **2019**, *151*, 214108]. We compute the magnetic exchange coupling constants using the spin projection and non projection approaches for sets of molecules composed of dinuclear and polynuclear H–He models, organic radical molecules, and chlorocuprate, and compare these results against accurate theories and experiment. Our results show that for the systems that mainly consist of single electron regions, PZSIC performs well but for more complex organic systems and the chlorocuprates, an overcorrecting tendency of PZSIC combined with the DFAs utilized in this work is more pronounced, and in such cases LSIC with kinetic energy density ratio performs better than PZSIC. Analysis of the results in terms of SIC corrections to the density and to the total energy shows that both density and energy correction are required to obtain an improved prediction of magnetic exchange couplings.

1 Introduction

The characterization of the magnetic properties of materials is crucial for applications such as memory storage devices, spintronics, quantum computing, and magnetic sensors. In many cases, the magnetic behavior arises from interactions between localized electrons typically described using model spin Hamiltonians, including spin-spin exchange and dipolar interactions, and magnetic anisotropy contributions. The accurate theoretical description of magnetic properties such as exchange interactions or spin levels by means of electronic structure calculations is especially challenging since the energy spacing involved can be much smaller than the typical electronic excitation energies. In particular, the calculation of magnetic exchange couplings (J) in transition metal complexes have been the focus of attention for density functional theory methods.^{1–6} In this respect, some approximations can be successful in predicting J couplings for certain type of complexes but fail for others. Hybrid density functional approximations, in their different flavors, and recently the strongly constrained appropriately normed (SCAN) meta-generalized-gradient-approximation functional

(meta-GGA), have shown some promise for predicting magnetic properties, including J couplings.^{7–10}

Experimentally, coupling parameters are obtained by fitting susceptibility data. For complex structures with multiple exchange pathways, this fitting can become very challenging or even impossible. Other experimental techniques, such as electron paramagnetic resonance (EPR), electron spin resonance (ESR), or inelastic neutron scattering (INS) are also used to determine exchange couplings, but they present the same type of shortcomings. Thus, for large, multi-center magnetic complexes, computational methods that can predict J couplings are the only choice to determine these constants. Electronic structure methods are routinely used to determine the coupling parameter by mapping energies of different spin states of spin Hamiltonians.^{11–14} Among electronic structure methods, density functional theory (DFT)^{15,16} is widely used because it provides a reasonable balance between accuracy and computational efficiency. For the case of multi-center transition metal complexes, computational efficiency becomes crucial, and therefore methods based on DFT are, many times, the only alternative. Unfortunately, approximations to the exchange-correlation functionals used in density functional calculations suffer from self-interaction error (SIE).^{17,18} This error emerges when the approximate exchange-correlation energy does not completely cancel out the Coulomb interaction of an electron with itself for one-electron systems. It is well documented that the presence of SIE hinders the accurate description of many properties involving chemical reactions, dissociation, charge transfer, and magnetism.^{19–23} The SIE in standard approximate functionals results in excessive electron delocalization, causing an error in predicted properties that is known as delocalization error.^{24–26} The Heisenberg exchange coupling parameters are very sensitive in sign and magnitude to the overlap between orbitals, both involving spin centers and bridging ligands,^{27–29} and hence the delocalization error, which affects the spin-density at the metal centers, gives rise to large changes in the sign and strength of the calculated coupling parameters J .

One approach to mitigate SIE in DFAs is to use hybrid functionals such as the hybrid ver-

sion of the Perdew-Burke-Ernzerhoff (PBEh)³⁰ or the popular B3LYP (Becke’s 3-parameter for exchange and Lee-Yang-Parr for correlation).³¹ Over the years several groups have documented the performance of various DFAs for J couplings.^{9,23,32–37} The general conclusions of these studies suggest that there is no single approach that performs best across different types of couplings involving different transition metals, and hence the predictive power of a particular DFA approach is limited. In view of this, other approaches based on DFT that can reduce SIE are specially attractive candidates for the prediction of J couplings.

Perdew and Zunger, in 1981, proposed a scheme (PZSIC) to explicitly remove the SIE on an orbital-by-orbital basis,¹⁷ making the approximate energy functional exact for any one-electron density (see Section 2). Their work extends the earlier self-interaction scheme for X - α exchange due to Lindgren³⁸ to the local density functional approximation. Ruiz *et al.*²³ studied the effect of SIE on exchange couplings using PZSIC to determine the J coupling in a simple model system, H–He–H. In recent years, the development of the Fermi-Löwdin orbital self-interaction correction (FLOSIC) methodology^{22,39–42} and software^{10,43–50} improved the accessibility of SI-free calculations. FLOSIC has been applied to study various molecular properties and showed improvement over LSDA and GGA for most cases where SIE dominates the errors.^{42,51–65} Joshi *et al.*⁵⁵ used FLOSIC with LSDA to investigate the effect of SIE on more realistic systems than the simple model H–He–H, and found that removing the SIE corrects J couplings towards more accurate methods such as hybrid density functionals and wave function based methods, in line with the earlier study of Ruiz *et al.*²³

It is well known that that PZSIC tends to overcorrect, particularly for the equilibrium properties, resulting in errors of opposite sign to those from semilocal functionals.^{66,67} Recently, Zope *et al.*⁶⁸ introduced the locally scaled SIC (LSIC), which uses a pointwise iso-orbital indicator to identify the one electron self-interaction regions in many-electron system (see Section 2.4) and to scale down the SIC in the many-electron regions. LSIC works well for both equilibrium properties as well as for properties that involve a stretched bond, and provides an improved performance with respect to standard SIC for a wide range of electronic

structure properties.^{61,65,69–71} Motivated by the success of LSIC, in this work we explore the potential of locally scaled SIC methods for the prediction of magnetic exchange coupling constants J . We also perform more comprehensive study of coupling constants by applying three different SIC methods to the three levels of exchange-correlation approximations that include the most recent r²SCAN meta-GGA functional. The two SIC methods besides the well known PZSIC method¹⁷ are the orbitalwise scaled down SIC method of Vydrov *et al.*⁶⁶ and the recent LSIC method of Zope and coworkers.⁶⁹ Results of various SIC methods for the three different class of systems are compared and analyzed.

2 Theory

2.1 Magnetic exchange coupling constants

Isotropic spin-spin interaction between two magnetic centers A and B are usually described by means of the Heisenberg-Dirac-Van Vleck (HDVV) spin Hamiltonian,⁷²

$$H_{HDVV} = - \sum_{A,B} J_{AB} \vec{S}_A \cdot \vec{S}_B, \quad (1)$$

where \vec{S}_A (\vec{S}_B) is the spin operator for the site A (B), and J_{AB} is the exchange coupling constant. The magnitude and sign of J_{AB} is related to the strength and the nature of the coupling (ferromagnetic or antiferromagnetic). To determine J couplings from electronic structure calculations, it is necessary to map the energy spectrum of the HDVV Hamiltonian to the electronic structure energy spectrum. To illustrate this, consider a two spin-1/2 case. The energy difference between the singlet or low-spin state $|\text{LS}\rangle = |S=0\rangle$ and any high-spin or triplet state $|\text{HS}\rangle = |S=1\rangle$ from the HDVV Hamiltonian is $E_{\text{HS}} - E_{\text{LS}} = J_{AB}$. However, for single-reference methods such as those based on DFT, the singlet state is not accessible. In these cases, one can resort to evaluating the energy difference between the broken-symmetry low-spin state $|\text{BS}\rangle = |\uparrow\downarrow\rangle$ and the high-spin (HS) state $|\text{HS}\rangle = |\uparrow\uparrow\rangle$, which for the two

spin-1/2 case is $E_{\text{BS}} - E_{\text{HS}} = J_{AB}/2$. This approach is exact for perfectly localized magnetic centers, and it can be generalized to two spins S_A and S_B to extract the exchange coupling as

$$J_{\text{SP}} = \frac{E_{\text{BS}} - E_{\text{HS}}}{2S_A S_B}, \quad (2)$$

where SP indicates spin-projected. This approach was introduced by Noodleman¹² and is widely used in the literature. For cases where there is significant overlap between the magnetic orbitals, one can use the $|\text{HS}\rangle$ and $|\text{LS}\rangle$ states to evaluate the expectation values of the HDVV Hamiltonian. This gives place to the non-projected (NP) approach of Ruiz *et al.*,⁷³ where

$$J_{\text{NP}} = \frac{E_{\text{LS}} - E_{\text{HS}}}{2S_A S_B + S_B}. \quad (3)$$

For single-reference states, this approach is exact for fully delocalized spins. It should also be mentioned, although it is not employed in this work, Yamaguchi's approach, which interpolates between both NP and SP approaches,⁷⁴

$$J_Y = \frac{2(E_{\text{BS}} - E_{\text{HS}})}{\langle S^2 \rangle_{\text{HS}} - \langle S^2 \rangle_{\text{BS}}}. \quad (4)$$

The relation between static correlation in the DFAs and SIE has been discussed in the literature.^{75–79} It has been argued that DFA calculations can contain spurious static correlation which causes the BS energy to correspond to the singlet state energy. This may be different when SIE is removed. Since the NP approach approximates the singlet energy with the BS energy, the bare DFA (SIE-uncorrected) NP approach can give better estimates of coupling constants while in the case of the SP approach this will result in double counting of the static correlation contributions.^{80,81}

2.2 PZSIC and FLOSIC

In the PZSIC¹⁷ method, the one-electron SIE is removed from the energy functional by subtracting the orbitalwise self-Hartree and self-exchange, and correlation as follows,

$$E^{PZSIC}[\rho_{\uparrow}, \rho_{\downarrow}] = E^{DFA}[\rho_{\uparrow}, \rho_{\downarrow}] - \sum_{i\sigma}^{occ} \{U[\rho_{i\sigma}] + E_{XC}^{DFA}[\rho_{i\sigma}, 0]\}, \quad (5)$$

where i and σ are the orbital and spin indices, and $\rho_{i\sigma}$ is the density for orbital $i\sigma$. In the traditional PZSIC approach, one solves the localization equations,⁸² to determine the set of localized orbitals that minimize the PZSIC total energy. The computational cost of solving localizations equation can be a limiting factor for practical applications due to its poor scaling.³⁹ In recent years, the FLOSIC approach^{22,39–41} for solving the PZSIC problem was proposed. FLOSIC is a size-extensive implementation of the PZSIC method, and its computational efficiency affords the study of large systems. In FLOSIC, using $3N$ positions in space (called Fermi-orbital descriptors, or FODs), \mathbf{a}_j , the set of KS orbitals ψ_i is transformed to a set of Fermi orbitals F_j as follows,⁸³

$$F_j(\mathbf{r}) = \frac{\sum_i \psi_i(\mathbf{a}_j) \psi_i(\mathbf{r})}{\sqrt{\rho(\mathbf{a}_j)}}. \quad (6)$$

The resulting Fermi orbitals are normalized but not necessarily orthogonal. The Löwdin orthogonalization scheme⁸⁴ is used to form a set of orthonormal Fermi-Löwdin orbitals (FLOs). The FLOs are then used to solve Eq. (5). Since FLOs depend on the FODs, minimizing the PZ energy with respect to the choice of localized orbitals is equivalent to finding the set of FODs that minimize the energy. Thus, the FLOSIC method requires optimizing the $3N$ \mathbf{a}_j parameters instead of N^2 parameters, as in the localization equation approach. For more details on the FLOSIC methodology, we refer the reader to Refs. 22,39–41.

2.3 Orbitalwise scaled SIC

PZSIC eliminates one-electron SIE and improves properties for which DFAs perform poorly due to SIE, but it also worsens the equilibrium properties where SI-uncorrected DFAs tend to perform well. This paradoxical behavior of PZSIC⁶⁷ is due to an over-correcting tendency of PZSIC in the many-electron region. In the orbital scaling approach (OSIC) of Vydrov *et.al.*,⁶⁶ an orbitalwise scaling factor $X_{i\sigma}$ is introduced in Eq. (5) to reduce the over-correction as follows,

$$E^{OSIC}[\rho_{\uparrow}, \rho_{\downarrow}] = E^{DFA}[\rho_{\uparrow}, \rho_{\downarrow}] - \sum_{i\sigma}^{occ} X_{i\sigma} \{U[\rho_{i\sigma}] + E_{XC}^{DFA}[\rho_{i\sigma}, 0]\}. \quad (7)$$

A quantity such as $\int \rho_i(\vec{r})\tau^W(\vec{r})/\tau(\vec{r})d\vec{r}$ may be used as the orbital scaling factor $X_{i\sigma}$ where τ and τ^W are the non-interacting (positive) and von Weizsäcker kinetic energy densities, respectively. Alternatively, $\int \rho_i(\vec{r})^2/\rho(\vec{r})d\vec{r}$ can also be used for $X_{i\sigma}$.⁸⁵ OSIC provides improvement over PZSIC for atomization energies but it reintroduces some errors corrected by the PZSIC scheme. For example, unlike in PZSIC, the dissociation of heteronuclear molecules in OSIC showed spurious fractional charge dissociation.⁸⁶

Unlike the OSIC and PZSIC methods, the recent LSIC method⁶⁹ described in the next section showed promising results for both the equilibrium properties as well as stretched bond properties when used in combination with the LSDA functional.

2.4 Local-scaling SIC methods

In the LSIC approach introduced by Zope *et al.*,⁶⁹ the magnitude of the SIC correction is determined locally (pointwise) in space using a local scaling factor $f(\vec{r})$, also known as iso-orbital indicator. Thus, the SIC energy in the the LSIC method is given by

$$E_{XC}^{LSIC-DFA}[\rho_{\uparrow}, \rho_{\downarrow}] = E_{XC}^{DFA}[\rho_{\uparrow}, \rho_{\downarrow}] - \sum_{i\sigma}^{occ} \{U^{LSIC}[\rho_{i\sigma}] + E_{XC}^{LSIC}[\rho_{i\sigma}, 0]\}, \quad (8)$$

where

$$U^{LSIC}[\rho_{i\sigma}] = \frac{1}{2} \int d\vec{r} f_{\sigma}(\vec{r}) \rho_{i\sigma}(\vec{r}) \int d\vec{r}' \frac{\rho_{i\sigma}(\vec{r}')}{|\vec{r} - \vec{r}'|} \quad (9)$$

and

$$E_{XC}^{LSIC}[\rho_{i\sigma}, 0] = \int d\vec{r} f_{\sigma}(\vec{r}) \rho_{i\sigma}(\vec{r}) \epsilon_{XC}^{DFA}([\rho_{i\sigma}, 0], \vec{r}) \quad (10)$$

are the scaled-down self-Hartree and self-exchange-correlation energies. In the original LSIC work,⁶⁹ Zope *et al.* used $z_{\sigma}(\vec{r}) = \tau_{\sigma}^W(\vec{r})/\tau_{\sigma}(\vec{r})$ for $f_{\sigma}(\vec{r})$. This iso-orbital indicator interpolates between the single-orbital regions ($z = 1$) and the uniform density regions ($z = 0$), and it is used as a weight for integrating the SIC energy densities accordingly. z_{σ} is not necessarily the only choice with LSIC, and other local scaling factors can be used and sometimes preferred.⁸⁷ Hereafter, we refer to LSIC with $z_{\sigma}(\vec{r}) = \tau_{\sigma}^W(\vec{r})/\tau_{\sigma}(\vec{r})$ as LSIC(z) and to LSIC with $w_{i\sigma}(\vec{r}) = \rho_{i\sigma}(\vec{r})/\rho_{\sigma}(\vec{r})$ as the weight factors as LSIC(w), and similarly for OSIC(z) and OSIC(w) for OSIC with the corresponding iso-orbital indicator. The LSIC method is implemented in the development version of the FLOSIC code.^{43,44}

3 Computational Details

All calculations in this work were performed with the development version of the FLOSIC code.^{43,44} The FLOSIC code is a software based on the UTEP-NRLMOL code and inherits the features of the original NRLMOL including the NRLMOL Gaussian-type orbital basis set⁸⁸ and adaptive integration mesh.⁸⁹ This code has the FLO implementation of PZSIC, OSIC, and LSIC. Hereafter, we refer to FLO-PZSIC, FLO-OSIC, and FLO-LSIC as PZSIC, OSIC, and LSIC for brevity. To make calculations attainable, in this work we employ a perturbative flavor of LSIC, where the PZSIC densities are utilized to evaluate the LSIC energy. In case of OSIC method we have found that one shot OSIC results to be practically

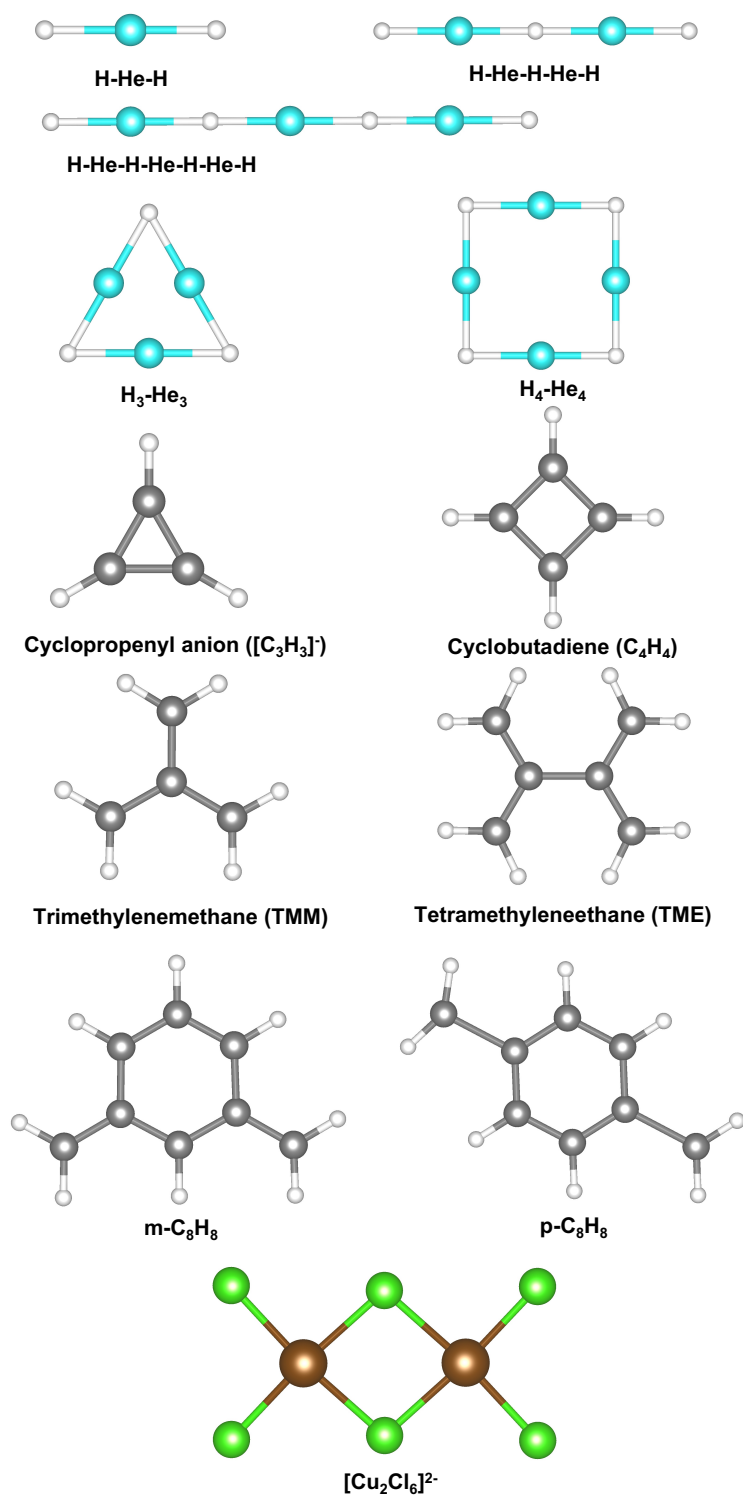


Figure 1: Molecular schemes used in this work for the evaluation of magnetic exchange couplings constants with self-interaction corrected methods. Hydrogen, helium, carbon, chlorine, copper atoms are color coded as white, cyan, gray, green, and brown, respectively.

same as fully self-consistent OSIC results.⁸⁷

We considered the following representative exchange-correlation functionals: the local spin density approximation (LSDA) parameterized by Perdew and Wang (PW92),⁹⁰ the Perdew-Burke-Ernzerhof (PBE)^{91,92} generalized gradient approximation (GGA) functional, and the strongly constrained and appropriately normed (SCAN)⁹³ and the recent r²SCAN meta-GGA⁹⁴ functionals. Since SCAN functional is numerically problematic, we used a very dense integration mesh (roughly 45000 grid points per atom for organic molecules) specifically tailored for this functional to obtain accurate energies.⁵³ Likewise, we used a mesh with an intermediate grid density between GGA and SCAN for r²SCAN calculations since meta-GGAs generally require finer meshes than GGAs.

The PZSIC is applied in combination with the LSDA, PBE and SCAN functionals. For the LSIC calculations, we considered only LSDA since LSIC combined with GGAs or meta-GGAs causes a gauge inconsistency problem.⁶⁸

We first assess FLOSIC and locally-scaled SIC methods for magnetic exchange coupling constants using $\text{H} \cdots \text{He}$ model systems, which were introduced to study magnetic exchange coupling parameters with different electronic structure methods, as well as representative realistic molecular systems, including a small transition metal complex. For all the $\text{H} \cdots \text{He}$ models reference values from accurate wave function calculations are available. We included a linear H-He-H molecule of three H-He distances $d = 1.25, 1.625$, and 2.00 \AA , two H-(He-H)_n chains with $n = 2$ and 3 , a triangle and a square (see Fig. 1). For all these model systems, the $1s$ hydrogen orbitals are coupled through a super-exchange mechanism mediated by the He orbitals. These simple super-exchange model systems were used multiple times in the literature to assess the performance of electronic structure methods for magnetic exchange couplings. The smallest linear H-He-H has been also used to address the effect of SIE on exchange coupling constants.²³ Additionally, we considered six organic bi-radical molecules: $[\text{C}_3\text{H}_3]^-$, C_4H_4 , trimethylenemethane (TMM), $p\text{-C}_8\text{H}_8$, $m\text{-C}_8\text{H}_8$, and tetramethyleneethane (TME), and chlorocuprate $[\text{Cu}_2\text{Cl}_6]^{2-}$ (shown in Fig. 1). The structures of $[\text{C}_3\text{H}_3]^-$ and

C_4H_4 were taken from Ref. 95, and the structures of p- C_8H_8 and m- C_8H_8 are from Ref. 96. The TMM and TME structures are taken from Ref. 55. The $[\text{Cu}_2\text{Cl}_6]^{2-}$ structure was taken from Ref. 97.

The NRLMOL Gaussian basis set was used for H/He models and the organic radical molecules.⁸⁸ For the $[\text{Cu}_2\text{Cl}_6]^{2-}$ complex, the Stuttgart relativistic small core effective core potential (ECP) consisting of 10 electrons was used in combination with its corresponding valence basis set^{98,99} for copper, and Stuttgart relativistic large core ECP was used for chlorine atoms. The Stuttgart basis set and ECP parameters were obtained from the Basis Set Exchange library.¹⁰⁰

The optimal FLOs in the FLOSIC calculations are obtained by minimizing the SIC energy with respect to the FOD positions. We used the conjugate gradient algorithm to optimize FOD positions. The force tolerance of $10^{-3}E_h/a_0$ was used for the organic and copper molecules. A tighter tolerance of $10^{-5}E_h/a_0$ was used for FOD optimization for the H-He complexes. A typical relaxed FOD structure has an FOD at the nuclear position corresponding to the 1s electrons for atoms other than one-electron systems. For carbon and oxygen, the valence FODs are found at the vertices of a tetrahedron centered at the corresponding nuclei for the hybridized $2s2p$ electrons. The valence electrons in the $3s3p3d$ shells in the copper atoms form symmetrical arrangements around the atomic centers. The set of optimized FOD used in this work is available on GitHub (https://github.com/FLOSIC/si_magnetic_exchange_coupling).

For the magnetic exchange coupling calculations, both J_{SP} and J_{NP} were obtained using Eqs. (2) and (3), where each E_{HS} and E_{BS} were calculated at the DFA, PZSIC-DFA, OSIC-DFA, and LSIC-DFA levels of theory. Since the HS and BS states have different orbital configurations (i.e. one for parallel and another for anti-parallel spins), in our FLOSIC calculations we obtained a distinct set of optimal FODs for each spin configuration: one corresponding to the HS state and the other to the BS state.

4 Results and Discussion

Table 1: Magnetic exchange coupling constants J_{SP} (in cm^{-1}) for H–He–H with the three H–He distances, d . J_{NP} is a half of J_{SP} . Mean absolute percentage deviations (MAPD) with respect to full-CI are also shown.

Method	d (Å)			MAPD(%)	
	1.25	1.625	2.00	SP	NP
LSDA	-12493	-1494	-159	183	41
PBE	-8672	-916	-88	74	13
SCAN	-8246	-948	-80	68	16
r ² SCAN	-8304	-956	-84	72	14
PZSIC-LSDA	-5503	-632	-61	17	42
PZSIC-PBE	-4894	-541	-51	1	50
PZSIC-SCAN	-5526	-606	-48	10	44
PZSIC-r ² SCAN	-5600	-633	-51	11	44
LSIC(z)-LSDA (perturbative)	-5734	-696	-76	33	34
LSIC(w)-LSDA (perturbative)	-4786	-429	-24	25	62
OSIC(z)-LSDA (perturbative)	-5820	-709	-77	35	33
OSIC(z)-LSDA (SCF)	-5775	-683	-60	22	39
OSIC(w)-LSDA (perturbative)	-5318	-590	-54	9	45
OSIC(w)-LSDA (SCF)	-5332	-606	-58	12	43
LSDA@PZSIC-LSDA	-8427	-1042	-109	94	9
PBE@PZSIC-PBE	-6599	-767	-76	42	28
SCAN@PZSIC-SCAN	-7240	-835	-71	48	25
r ² SCAN@PZSIC-r ² SCAN	-7213	-845	-74	50	24
Full-CI ^a	-4860	-544	-50	—	—

^aReference 97

4.1 H–He–H model

For the linear H–He–H model system, we considered three different H–He bond distances ($d = 1.25, 1.625, \text{ and } 2.00$ Å) as mentioned in Sec. 3 with the LSDA, PBE, and SCAN and r²SCAN meta-GGAs functionals and their SIC counterparts. In Table 1, we show the calculated J_{SP} for the H–He–H model with DFAs, PZSIC-DFAs, LSIC, OSIC, DFA@PZSIC-DFA, where DFA@PZSIC-DFA denotes PZSIC density with a DFA, and reference full-configuration interaction values.⁹⁷ The mean absolute percentage deviations (MAPD) for

each method are also included in Table 1. It should be mentioned that for this system, the SP method to map exchange couplings is physically more meaningful than the NP since it takes into account the broken spin symmetry nature of the low-spin state. By contrast, the NP approach assumes that the broken symmetry state provides the correct energy of the low spin state. Since in this case the spin magnetization is very localized at the H centers, the SP method is expected to yield the correct mapping. The NP values are half of the SP values for this system and therefore are not shown. Typically, DFA exchange couplings using SP formulation are overestimated, and their J_{NP} values are therefore closer to experimental values.³⁵

For all the four DFA functionals employed here, we find that the J_{SP} values are larger by a factor of 2 – 3 compared to the reference values. When SIE are removed using PZSIC, the predicted antiferromagnetic coupling strengths decrease, resulting in reduction in the deviations in all three cases. J_{SP} ’s obtained with PZSIC-PBE show the smallest MAPD, with results comparable to the full-CI reference values.

A graphical comparison of the percentage deviations of J_{SP} ’s is shown in Fig. 2. PZSIC with the four DFAs shows fairly good performance with relatively small deviations (MAPD, 1 – 17%). The reduction of J_{SP} with PZSIC is partly due to an improved electron density. To examine the effect of PZSIC density, we calculated the J_{SP} parameters using the PZSIC density with the DFAs (herein DFA@PZSIC-DFA). The calculated DFA@PZSIC-DFA values are also shown in Table 1. All the DFA@PZSIC-DFA values are intermediate between respective DFA and PZSIC-DFA values. Moreover, the comparison of DFA errors with DFA@PZSIC-DFA errors shows that the density correction accounts for 17 – 49% of the errors in DFA-only calculations going from r²SCAN to LSDA. Thus the density correction plays a significant part in improving the results particularly for LSDA and GGA functionals which belong to the lower rungs of Jacob ladder of density functionals.¹⁰¹ The rest of the correction in PZSIC arises from the correction to the energy functional. Since the H–He–H system consists of mostly single electron regions where PZSIC is exact, PZSIC performs well

for J_{SP} for this set of systems. On the other hand, the LSIC(z), LSIC(w) and OSIC(z) methods surprisingly perform much worse compared to PZSIC. LSIC methods are applied perturbatively on PZSIC density and therefore the higher errors in these results stem from the functional alone. LSIC mimics PZSIC in the one-electron regions but reduces the corrections in the many-electron regions. As LSIC reduces the SIC energy correction with respect to PZSIC, the LSIC total energies are higher than the PZSIC total energies. This energy shift is larger on the HS states than the BS states, and hence LSIC shows larger values of the coupling constant than PZSIC. The best performance for this system comes from the OSIC(w) method. The w factor identifies the weak interaction regions better compared to the z factor which may have contributed to the better performance of the OSIC(w).

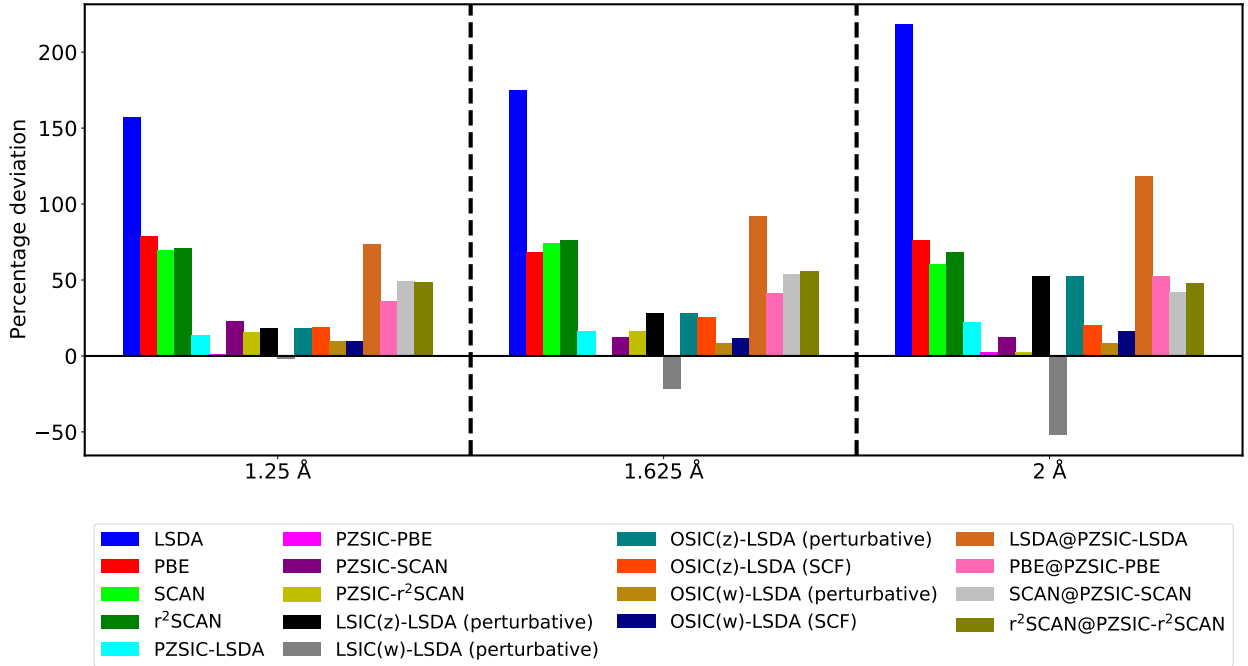


Figure 2: Percentage deviations of $|J_{SP}|$ for H-He-H with respect to the CI values.

In the next sections, we investigated systems that involve many-electron regions where PZSIC may show overcorrections.

4.2 H...He multicenter models

Next, we assessed J couplings with SIE-free DFAs on a set of multi-center H...He model systems the structures of which are shown in Fig. 1. These complexes are extensions of the two-center H–He–H for which accurate wave function as well as hybrid functional calculations are available.¹⁰² Here, we studied the four multi-center complexes: H₃He₂, H₄He₃, H₃He₃, and H₄He₄. The structures of these complexes are taken from Ref. 102. The bond distances between H...He were fixed to 1.625Å in all four cases. For the evaluation of J_{SP} couplings, Eq. (1) can be easily extended to multicenter spin cases.¹⁰² The equations used to determine the coupling constants of the multicenter complexes can be found in supplementary information.

Our calculated J_{ij} for the nearest and the second nearest neighbor interactions with DFAs, PZSIC-DFAs, and LSIC are presented and compared against the available CASPT2 values in Table 2. All four DFAs overestimate J_{SP} with LSDA having the largest errors. The mean absolute percentage deviations for PBE, SCAN, and r²SCAN are comparable. The first nearest neighbor couplings (J_{SP}^{12} and J_{SP}^{23}) tend to show smaller absolute percentage deviations than the second nearest neighbor couplings (J_{SP}^{13}) because the relative uncertainties are small. Removing SIE with PZSIC systematically reduces these deviations with MAPDs of 27, 24, and 38% for PZSIC-LSDA, -PBE, and -SCAN, respectively. On the other hand, LSIC(z) tends to increase the coupling strengths for the nearest neighbor pairs and thus results in overestimation, consistent with what we observed for the linear H–He–H. For the second nearest neighbor pairs, which are weakly coupled, LSIC(z) tends to improve the coupling strengths over PZSIC. On the other hand, LSIC(w) tends to underestimate the coupling in general and even leads to ferromagnetic coupling for the next nearest neighbors. Interestingly, when MAPDs are compared, the density based OSIC(w) method shows the smallest percentage deviation of 14% among the SIC calculations. No systematic improvement is seen for the OSIC(z) method. Overall, PZSIC-PBE and OSIC(w) performs well for this set of toy systems.

Table 2: Magnetic exchange coupling constants J_{SP} (in cm^{-1}) for the $\text{H}\cdots\text{He}$ multicenter complexes. The bond length $\text{H}\cdots\text{He}$ is fixed to 1.625 Å in all cases. Structures are shown in Fig. 1.

System		DFA				PZSIC			LSIC(z)	LSIC(w)	OSIC(z)		OSIC(w)		Ref. ^a
		LSDA	PBE	SCAN	r ² SCAN	LSDA	PBE	SCAN	LSDA ^b	LSDA ^b	LSDA ^b	LSDA	LSDA ^b	LSDA	
H_3He_2	J_{12}	-1673	-1045	-994	-1019	-682	-600	-670	-744	-467	-763	-735	-633	-647	-586
	J_{13}	-41.3	-6.7	-8.4	-8.9	-3.0	-1.8	-2.0	-3.2	-1.4	-2.8	-4.8	-2.5	-2.9	-4.0
H_4He_3	J_{12}	-1687	-1049	-1000	-1025	-684	-602	-662	-747	-480	-766	-740	-636	-650	-587
	J_{23}	-1830	-1188	-1036	-1060	-733	-660	-702	-786	-494	-812	-781	-681	-696	-629
	J_{13}	-44.5	-6.9	-7.3	-7.8	-4.7	-2.3	-6.6	-3.0	10.0	-3.4	32.6	-3.7	-3.9	-3.4
H_3He_3	J_{12}	-442	-314	-305	-311	-230	-221	-228	-263	-193	-274	-239	-231	-235	-197
H_4He_4	J_{12}	-1425	-917	-838	-849	-611	-540	-576	-606	-412	-651	-619	-558	-569	-516
	J_{13}	-22.3	0.5	-1.5	-1.5	-2.5	-1.6	-0.5	-7.2	6.0	-4.3	30.7	-7.5	-9.2	-8.8
MAPD	SP	395	82	79	84	27	24	38	23	89	30	206	14	14	–
	NP	147	22	24	25	48	59	49	45	94	45	136	50	47	–
MAD	SP	579	252	209	221	54	15	42	79	62	95	84	28	36	–
	NP	131	34	55	49	132	152	138	119	189	112	125	144	141	–

^aCASPT2 values from Ref. 102

^bPerturbative calculation using PZSIC-LSDA densities.

4.3 Organic radical molecules

In this section, we assess the performance of SIC approximations for J couplings on a set of six organic radical molecules, $[\text{C}_3\text{H}_3]^-$, C_4H_4 , trimethylenemethane (TMM), $p\text{-C}_8\text{H}_8$, $m\text{-C}_8\text{H}_8$, and tetramethyleneethane (TME) (Fig. 1). This set is the same set used in the work of Joshi *et al.* where FLOSIC-LSDA was used to investigate the effects of SIE on exchange coupling constants.⁵⁵ We used the same methods as in the previous Section 2, with the exchange couplings in this case compared against available multireference configuration interaction or multi-reference perturbation theories such as CASSCF.^{95,103–106} The results are summarized in Table 3. The SP approach assumes that the energies of the electronic single-reference states can be mapped to the energies of broken-symmetry spin states, which is a physically acceptable assumption for the $\text{H}\cdots\text{He}$ complexes with localized electrons. This is not the case for the organic complexes, since the spin density is mostly delocalized. Hence, for these organic radical molecules, the NP mapping, which assumes that the electronic single-reference states provide a reasonable energy for the actual multi-reference states, is more physically acceptable. In Table 3 we show J_{SP} values (J_{NP} values are half as large as the

J_{SP} values). The MAPDs of both approaches are shown.

Similar to the results of the $\text{H}\cdots\text{He}$ systems, the DFA errors for the organic complexes too are large with MAPDs ranging from 60% for LSDA to 24% for SCAN. PZSIC improves the results, but the improvement is not consistent for all the DFAs employed here. While significant improvements are seen for LDA and PBE with PZSIC resulting in MAPDs of 14 and 12%, SCAN performance deteriorates to MAPD of 33%. With PZSIC-DFA, the strength of the interaction (either ferro or antiferromagnetic) is enhanced with respect to the parent DFAs couplings except for TME with PZSIC-LSDA. It is interesting to observe that the scaled SIC methods assessed here affect exchange couplings in a non-systematic way when compared to non-scaled PZSIC. The signs of the coupling constant are consistent with the reference values with DFAs, PZSIC-DFAs, LSIC(z), LSIC(w), and OSIC(w) but not with OSCI(z). For $\text{p-C}_8\text{H}_8$, OSIC(z) favors ferromagnetic coupling while the reference results favor antiferromagnetic coupling. The coupling strengths are generally enhanced with LSIC(z), LSIC(w) and OSIC(w) for all molecules except TME for which all the scaled SIC methods show lower strength compared to LSDA. Fig. 3 shows the percentage deviation between the computed $|J_{NP}|$ with DFA, PZSIC-DFA, LSIC, and OSIC and the corresponding reference values for each molecule. We also compared the coupling constants calculated using the DFA@PZSIC-DFA approach with the reference data in Table 4. These results show that the SIC to the density correction has little influence on the results with LSDA and PBE. The use of the SIC density in these functionals provide marginal improvement in MAPD of 1 and 3%, respectively. It is clear however that using SIC density in more accurate functionals such as SCAN and r^2SCAN results in appreciable reduction in MAPD by 9 and 16%.

4.4 Hexa-Chlorocuprate $[\text{Cu}_2\text{Cl}_6]^{2-}$

The hexa-chlorocuprate complex has two Cu(II) bridged with chlorine ligands, as shown in Fig. 4, with each copper atom in a $3d^9$ electron configuration that effectively acts as a spin $S = 1/2$ site. Experimentally, the chlorocuprate $[\text{Cu}_2\text{Cl}_6]^{2-}$ complex is found to be

Table 3: Calculated magnetic exchange coupling constants J_{SP} (in cm^{-1}) where J_{NP} is half the J_{SP} for a set of organic radical molecules.

System	DFA				PZSIC			LSIC(z)	LSIC(w)	OSIC(z)		OSIC(w)		Ref.
	LSDA	PBE	SCAN	r ² SCAN	LSDA	PBE	SCAN	LSDA ^a	LSDA ^a	LSDA ^a	LSDA	LSDA ^a	LSDA	
[C ₃ H ₃] [−]	3759	4506	6286	5974	6990	7004	8490	3610	6923	4712	4720	5406	5382	4547 ^b
C ₄ H ₄	-88	-1306	-4704	-4546	-6940	-7868	-9084	-2734	-538	-2945	-2653	-2508	-2154	-2833 ^b
TMM	4798	6448	11022	9982	11487	12470	14052	8078	8196	8614	8488	8484	8294	6121 ^c
p-C ₈ H ₈	-2710	-1916	-2816	-1666	-4816	-4662	-8308	-3258	-6573	922	1367	-7302	-8162	-2333 ^d
m-C ₈ H ₈	2276	3146	8176	5580	11904	13078	15212	6136	7134	7102	6536	8194	7668	6824 ^e
TME	-2838	-2198	-2614	-2516	-1948	-2486	-3036	-1260	-938	-1534	-1668	-1562	-1660	-1224 ^f
MAPD	SP	58	35	56	51	87	105	161	18	63	36	41	55	63
	NP	60	53	24	33	14	12	33	47	50	55	58	43	48

^aEvaluated using the PZSIC-LSDA density

^bCASSCF-MkCCSD from reference 95

^cCASPT2N from reference 103

^dAM1-CI from reference 105

^eCASSCF from reference 106

^fDDCI from reference 104

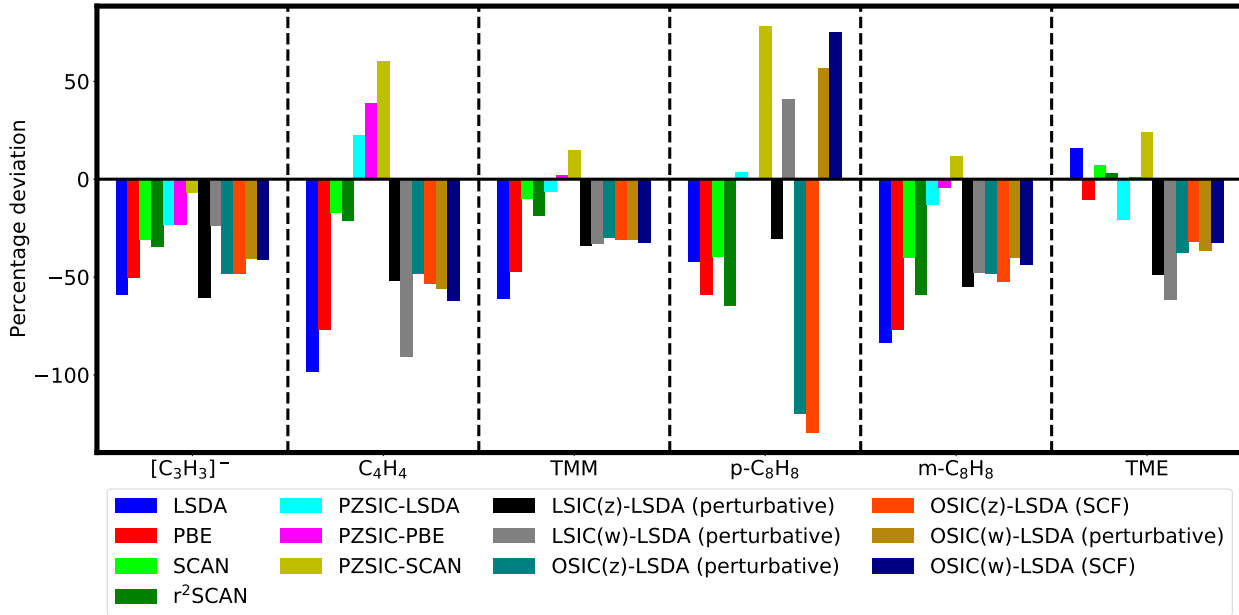


Figure 3: Percentage deviation of $|J_{NP}|$ for the set of six organic systems with respect to multi-configuration calculations.

Table 4: Calculated magnetic exchange coupling constants J_{SP} in cm^{-1} using DFA@PZSIC-DFA for the set of organic radical molecules.

System	LSDA@PZSIC-LSDA	PBE@PZSIC-PBE	SCAN@PZSIC-SCAN	r ² SCAN@PZSIC-LSDA
$[\text{C}_3\text{H}_3]^-$	4001	5024	6466	5712
C_4H_4	-713	-2340	-5408	-5342
TMM	5902	7638	10866	9748
p- C_8H_8	-2557	-1308	-3464	-4506
m- C_8H_8	4896	6596	15031	9274
TME	-1305	1494	-2686	-2396
MAPD	SP	22	83	66
	NP	59	15	17

weakly antiferromagnetic.¹⁰⁷ The magnetic susceptibility analysis of this complex shows that its magnetic character changes when outer non-bridging chlorine atoms are twisted around the Cu-Cu axis by an angle θ (see Fig. 4).¹⁰⁸ As θ varies from 0° to 45° , the coupling changes from being weakly antiferromagnetic to ferromagnetic. This change in the nature of the magnetic interaction with the angle θ makes the evaluation of the exchange coupling particularly challenging for DFT methods. Relative to the other organic complexes and the H-He model systems studied in this work, the d electrons in this complex are expected to be largely affected by the SIEs, making the hexa-chlorocuprate an interesting case to study the effect of SIE removal on magnetic exchange couplings. To this end, we use two structures taken from the literature.^{97,97,109} The first structure is the planar $[\text{Cu}_2\text{Cl}_6]^{2-}$ ($\theta = 0^\circ$)^{97,109} for which experiments show that the J values are between 0 to -40 cm^{-1} , indicating that the Cu(II) ions are weakly antiferromagnetically coupled.¹⁰⁷ This antiferromagnetic coupling constant is close to the value determined with PBE functional for Cu_3 complex in which case the Cu atoms are further apart.¹¹⁰ The second structure for $[\text{Cu}_2\text{Cl}_6]^{2-}$ ($\theta = 45^\circ$) was taken from Bencini *et al.*,⁹⁷ where the experimental coupling was found between 80 and 90 cm^{-1} . This qualitative change in the magnetic interaction with the twisting angle has also confirmed by *ab initio* methods (see Table 5).¹⁰⁸ We note that a slightly different planar structure was used in a previous FLOSIC-LSDA study.¹⁰⁹

The results of our calculations are summarized in Table 5. For the $\theta = 0^\circ$ configuration,

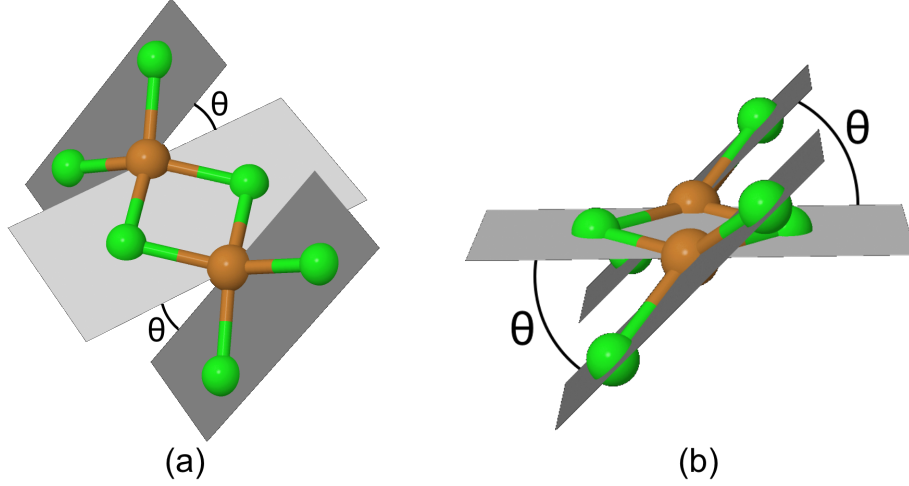


Figure 4: The structure of chlorocuprate $[\text{Cu}_2\text{Cl}_6]^{2-}$ where the outer CuCl_2 planes are twisted by angle θ with respect to the plane made by the inner Cu_2Cl_2 square: (a) top down view and (b) side view.

most methods give an antiferromagnetic interaction, with the exception of the OSIC with scaling factor w . In some of the SIC cases, the interaction strength is exaggerated, but never at the level of LSDA or PBE. It is interesting to point out that using the PZSIC densities with their parent DFA largely reduces the strength of the coupling for LSDA and PBE and only minimally affects the SCAN results. From the scaled methods, the orbital scaled and local scaled SIC LSDA yield similar small antiferromagnetic couplings, in line with the experimental and ab initio results. Turning to the $\theta = 45^\circ$ conformation, we found that while most methods predict a ferromagnetic coupling (the exceptions are PZSIC-LSDA and PZSIC-PBE), in some cases the couplings are largely overestimated. Here again the orbital scaled and local scaled SIC LSDA give J couplings in the range of the reference data.

Although for $\theta = 0^\circ$ configuration SCAN and r²SCAN predict coupling constants within the experimental range of values, these results are not completely reliable as for these self-interaction uncorrected functionals, the highest-occupied valence electron(s) are not bound as evidenced from the eigenvalue spectra shown in Fig. 5. It can be seen that removal of SIE results in the binding of the valence electrons and thereby providing significantly better description of the electron density compared to the bare DFAs. The SIC fixes the

excessive electron delocalization in the uncorrected DFAs as evidenced in the localization of spin-densities on the Cu atoms as summarized in Table 6. These spin-populations were obtained from the Mulliken and Löwdin population analysis and by integrating the spin densities in atomic spheres of van der Waal radii placed on Cu sites.^{6,111} Interestingly, the spin populations also systematically increase in the corrected functionals from LSDA to PBE-GGA to SCAN meta-GGA.

Among all the variations of scaled SIC methods analyzed, only LSIC(z)-LSDA, OSIC(z)-LSDA are able to capture the correct nature and strength of the magnetic interaction for $\theta = 0^\circ$ and $\theta = 45^\circ$. This is encouraging since these methods (especially) LSIC also perform very well for other properties such as molecular dissociation energies and electric polarizabilities.^{61,68,71} On the other hand, within the non-scaled SIC methods, SCAN@PZSIC-SCAN and all the r²SCAN@PZSIC-DFA methods also successfully reproduce the magnetic interactions. This is an indication that the SIC densities are in general of better quality than their non-corrected counterparts, and these densities used with a “higher-rung” energy density functional are a good option for the evaluation of magnetic exchange couplings.

5 Conclusion

We have studied the magnetic exchange coupling parameters for sets of molecules: H–He models, six organic radical molecules, and $[\text{Cu}_2\text{Cl}_6]^{2-}$ using DFAs with and without SIC scheme of PZSIC. In addition, we assessed the impact of orbital-scaled SIC methods, such as OSIC and LSIC applied to LSDA to study the performance of these SIC methods on calculating the said property. For the H–He–H system using the SP method, application of PZSIC improves the resulting exchange couplings especially for PZSIC-PBE. With LSIC-LSDA, performance is slightly worsened compared to PZSIC-LSDA. For the H–He multi-nuclear systems, we find that removing SIE decreases coupling strengths. PZSIC shows good performance for the three functionals. LSIC(z)-LSDA shows slightly larger discrepancies

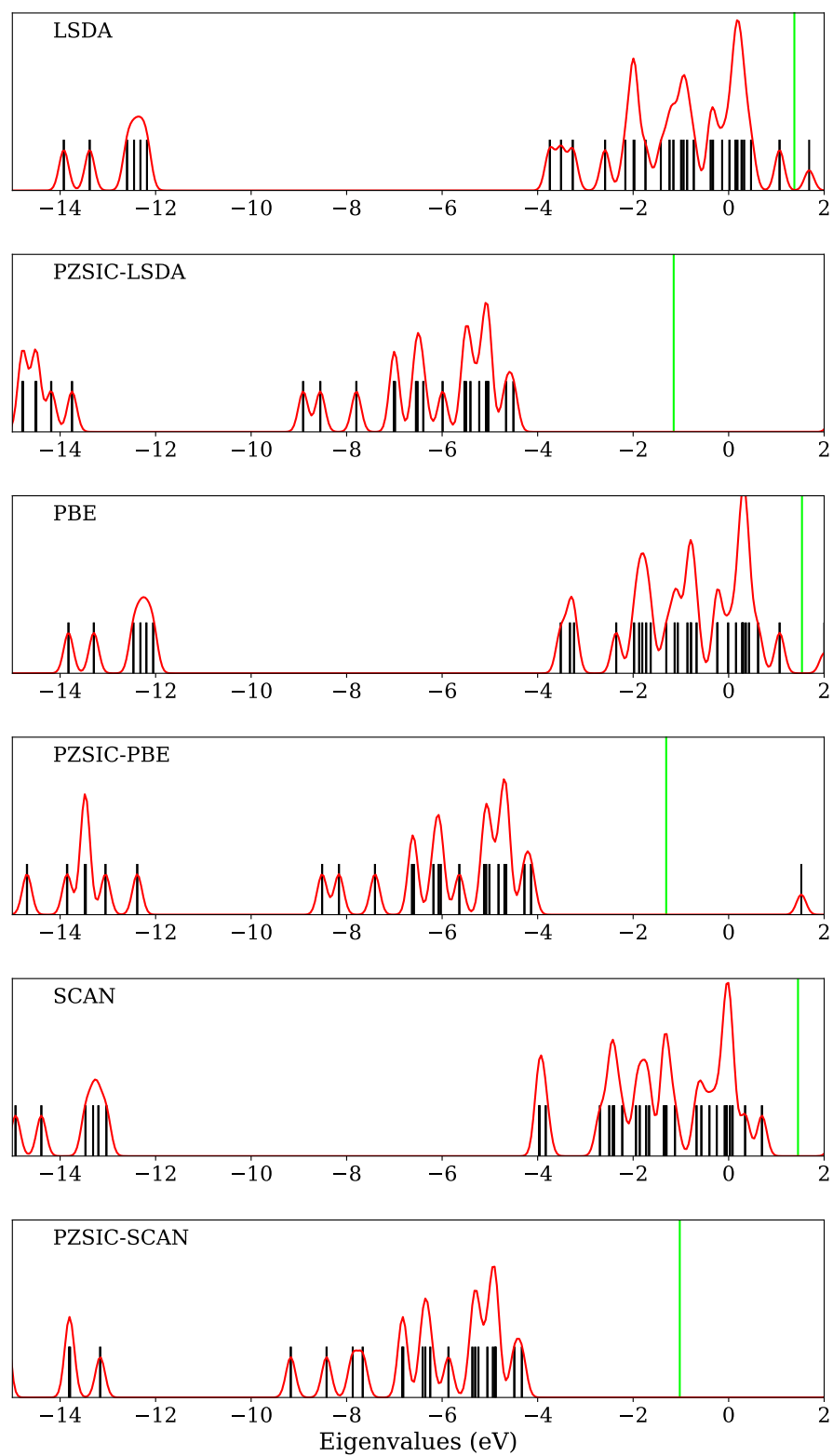


Figure 5: The eigenvalue spectra (in eV) of chlorocuprate $[\text{Cu}_2\text{Cl}_6]^{2-}$ in BS states. The green lines indicate the energy levels in between HOMO and LUMO eigenvalues.

Table 5: Magnetic exchange coupling constant J_{SP} (where J_{NP} is a half of J_{SP}) in cm^{-1} of the $[\text{Cu}_2\text{Cl}_6]^{-2}$ molecule.

Method	$\theta = 0^\circ$	$\theta = 45^\circ$
LSDA	-354	221
PBE	-234	150
SCAN	-3	159
$r^2\text{SCAN}$	-42	177
PZSIC-LSDA	-78	-12
PZSIC-PBE	-94	-24
PZSIC-SCAN	-99	228
LSIC(z)-LSDA ^a	-3	102
LSIC(w)-LSDA ^a	104	179
OSIC(z)-LSDA ^a	-15	107
OSIC(z)-LSDA(SCF)	-132	71
OSIC(w)-LSDA ^a	145	202
OSIC(w)-LSDA(SCF)	50	102
LSDA@PZSIC-LSDA	-131	59
PBE@PZSIC-PBE	-138	80
SCAN@PZSIC-SCAN	-25	87
$r^2\text{SCAN@PZSIC-LSDA}$	-49	76
$r^2\text{SCAN@PZSIC-PBE}$	-87	107
$r^2\text{SCAN@PZSIC-SCAN}$	-40	88
Ab initio, LOC ^b	-36	58
Ab initio, DELOC ^b	-6	47
Expt.	0 to -40 ^c	80 to 90 ^d

^aPerturbative calculation on PZSIC-LSDA density

^bReferences 112,113

^cReference 107

^dReference 108

than PZSIC-LSDA for the nearest-neighbor couplings but shows better agreement for the second nearest-neighbor couplings with the reference, resulting in a relatively small MAPD for this set. The smallest MAPD is seen in the density based OSIC(w)-LSDA with SP and PZSIC-PBE with NP. For the set of organic molecules, J_{SP} of uncorrected DFAs shows a fair performance while removing SIE overestimates the values notably. However, J_{NP} from PZSIC-DFAs coincidentally provides good agreement with the references where PZSIC-PBE and PZSIC-LSDA show two of the smallest percentage deviations. Although we find that the J_{NP} approach with LSIC and OSIC performs rather poorly, the J_{SP} approach combined with LSIC(z)-LSDA provides the best estimate among all SP approaches (MAPD, 18%)

Table 6: Spin density analysis of the $[\text{Cu}_2\text{Cl}_6]^{-2}$ molecule. $\int(\rho_\uparrow(\vec{r}) - \rho_\downarrow(\vec{r}))d\vec{r}$ of BS states at the one of the copper atom is shown. Similar results are found for HS states.

Method	$\theta = 0^\circ$			$\theta = 45^\circ$		
	Mulliken	Löwdin	Atom sphere	Mulliken	Löwdin	Atom sphere
LSDA	0.41	0.48	0.44	0.45	0.51	0.48
PBE	0.46	0.53	0.49	0.49	0.55	0.52
SCAN	0.54	0.61	0.58	0.57	0.63	0.61
r ² SCAN	0.52	0.59	0.57	0.55	0.61	0.59
PZSIC-LSDA	0.73	0.79	0.78	0.77	0.81	0.80
PZSIC-PBE	0.78	0.82	0.81	0.81	0.85	0.84
PZSIC-SCAN	0.76	0.80	0.78	0.80	0.83	0.82

in terms of percentage deviations (MAPD of the rest of the methods ranging 35 – 161%) where the triplet-singlet energy gaps of PZSIC are reduced in all six systems. Finally, for the chlorocuprate $[\text{Cu}_2\text{Cl}_6]^{2-}$, LSIC(z)-LSDA, SCAN, and r²SCAN produce very weak antiferromagnetic couplings for $\theta = 0^\circ$ and ferromagnetic coupling for $\theta = 45^\circ$ showing close agreement with experiments. Our DFA@PZSIC-DFA results are, in general, better than those of uncorrected DFAs but not as good as PZSIC-DFAs. Thus it seems that using an SIC density only is not sufficient and that an SIC energy correction is also needed for this property. Among the uncorrected DFAs, SCAN outperforms than LSDA and PBE in all cases. Also, r²SCAN closely mimics the SCAN functional. It is a good efficient alternative to SCAN due to its numerical efficiency. In all cases, we observed that LSIC reduces the amount of SIC from PZSIC, but this reduction does not always improve the magnetic exchange couplings. This is especially true for the systems that mainly consist of single electron regions where PZSIC already performs well. For the more complex organic systems and $[\text{Cu}_2\text{Cl}_6]^{2-}$, an overcorrecting nature of PZSIC is more pronounced when the SP approach is considered. We find that removing excess SIC using LSIC(z) gives an improved performance over PZSIC in these cases.

In a case-by-case performance, combinations of certain functionals and SP/NP approaches work very well for a set of systems but work rather poorly for others. This includes J_{SP} of PZSIC-PBE, -SCAN, and -r²SCAN on H-He-H, J_{NP} of PZSIC-PBE and J_{SP} of OSIC(w)-

LSDA on $\text{H}\cdots\text{He}$ multicenter complexes, J_{NP} of PZSIC-LSDA and PZSIC-PBE on organic molecules, and SCAN and r²SCAN on chrolocuprate. Thus, some care must be exerted prior to the practical application of these methods for the evaluation of magnetic exchange couplings. On the other hand, we find that the SP approach with LSIC(z)-LSDA provides a decently good overall performance across all four sets of systems, ranging from above average to a few of the best performances. This singles out the LSIC(z) method as a promising option for applications to exchange coupling constants in a wide range of systems. The performance of LSIC method can possibly be improved further by identifying more suitable iso-orbital indicator.

Supporting Information Available

- The equations used to determine the coupling constants of the $\text{H}\cdots\text{He}$ multicenter complexes

Acknowledgement

Authors acknowledge Drs. Luis Basurto and Carlos Diaz for discussions and technical support and Prof. Mark R. Pederson for comments on the manuscript. This work was supported by the US Department of Energy, Office of Science, Office of Basic Energy Sciences, as part of the Computational Chemical Sciences Program under Award No. DE-SC0018331. Support for computational time at the Texas Advanced Computing Center and at NERSC is gratefully acknowledged.

References

- (1) Rudra, I.; Wu, Q.; Van Voorhis, T. Accurate magnetic exchange couplings in transition-metal complexes from constrained density-functional theory. *J. Chem. Phys.*

2006, *124*, 024103.

- (2) Ruiz, E.; Rodríguez-Fortea, A.; Tercero, J.; Cauchy, T.; Massobrio, C. Exchange coupling in transition-metal complexes via density-functional theory: Comparison and reliability of different basis set approaches. *J. Chem. Phys.* **2005**, *123*, 074102.
- (3) Joshi, R. P.; Phillips, J. J.; Mitchell, K. J.; Christou, G.; Jackson, K. A.; Peralta, J. E. Accuracy of density functional theory methods for the calculation of magnetic exchange couplings in binuclear iron(III) complexes. *Polyhedron* **2020**, *176*, 114194.
- (4) Melo, J. I.; Phillips, J. J.; Peralta, J. E. Structural dependence of magnetic exchange coupling parameters in transition-metal complexes. *Chem. Phys. Lett.* **2013**, *557*, 110–113.
- (5) Phillips, J. J.; Peralta, J. E.; Christou, G. Magnetic Couplings in Spin Frustrated Fe_7^{III} Disklike Clusters. *J. Chem. Theory Comput.* **2013**, *9*, 5585–5589.
- (6) Postnikov, A. V.; Kortus, J.; Pederson, M. R. Density functional studies of molecular magnets. *Phys. Status Solidi (b)* **2006**, *243*, 2533–2572.
- (7) Ruiz, E.; Alemany, P.; Alvarez, S.; Cano, J. Toward the Prediction of Magnetic Coupling in Molecular Systems: Hydroxo- and Alkoxo-Bridged Cu(II) Binuclear Complexes. *J. Am. Chem. Soc.* **1997**, *119*, 1297–1303.
- (8) Bovi, D.; Guidoni, L. Magnetic coupling constants and vibrational frequencies by extended broken symmetry approach with hybrid functionals. *J. Chem. Phys.* **2012**, *137*, 114107.
- (9) Pantazis, D. A. Assessment of Double-Hybrid Density Functional Theory for Magnetic Exchange Coupling in Manganese Complexes. *Inorganics* **2019**, *7*, 57.
- (10) Yamamoto, Y.; Salcedo, A.; Diaz, C. M.; Alam, M. S.; Baruah, T.; Zope, R. R. Assessing the effect of regularization on the molecular properties predicted by SCAN

- and self-interaction corrected SCAN meta-GGA. *Phys. Chem. Chem. Phys.* **2020**, *22*, 18060–18070.
- (11) Hay, P. J.; Thibault, J. C.; Hoffmann, R. Orbital interactions in metal dimer complexes. *J. Am. Chem. Soc.* **1975**, *97*, 4884–4899.
 - (12) Noodleman, L. Valence bond description of antiferromagnetic coupling in transition metal dimers. *J. Chem. Phys.* **1981**, *74*, 5737–5743.
 - (13) Noodleman, L.; Case, D. A. In *Density-Functional Theory of Spin Polarization and Spin Coupling in Iron-Sulfur Clusters*; Cammack, R., Ed.; Advances in Inorganic Chemistry; Academic Press, 1992; Vol. 38; pp 423–470.
 - (14) Noodleman, L.; Peng, C.; Case, D.; Mouesca, J.-M. Orbital interactions, electron delocalization and spin coupling in iron-sulfur clusters. *Coord. Chem. Rev.* **1995**, *144*, 199–244.
 - (15) Hohenberg, P.; Kohn, W. Inhomogeneous Electron Gas. *Phys. Rev.* **1964**, *136*, B864–B871.
 - (16) Kohn, W.; Sham, L. J. Self-consistent equations including exchange and correlation effects. *Phys. Rev.* **1965**, *140*, A1133.
 - (17) Perdew, J. P.; Zunger, A. Self-interaction correction to density-functional approximations for many-electron systems. *Phys. Rev. B* **1981**, *23*, 5048–5079.
 - (18) Zunger, A.; Perdew, J.; Oliver, G. A self-interaction corrected approach to many-electron systems: Beyond the local spin density approximation. *Solid State Commun.* **1980**, *34*, 933–936.
 - (19) Patchkovskii, S.; Ziegler, T. Improving “difficult” reaction barriers with self-interaction corrected density functional theory. *J. Chem. Phys.* **2002**, *116*, 7806–7813.

- (20) Gräfenstein, J.; Kraka, E.; Cremer, D. The impact of the self-interaction error on the density functional theory description of dissociating radical cations: Ionic and covalent dissociation limits. *J. Chem. Phys.* **2004**, *120*, 524–539.
- (21) Dreuw, A.; Head-Gordon, M. Failure of Time-Dependent Density Functional Theory for Long-Range Charge-Transfer Excited States: The Zinobacteriochlorin-Bacteriochlorin and Bacteriochlorophyll-Spheroidene Complexes. *J. Am. Chem. Soc.* **2004**, *126*, 4007–4016.
- (22) Pederson, M. R.; Baruah, T. In *Adv. At. Mol. Opt. Phys.*; Arimondo, E., Lin, C. C., Yelin, S. F., Eds.; Academic Press, 2015; Vol. 64; pp 153–180.
- (23) Ruiz, E.; Alvarez, S.; Cano, J.; Polo, V. About the calculation of exchange coupling constants using density-functional theory: The role of the self-interaction error. *J. Chem. Phys.* **2005**, *123*, 164110.
- (24) Zhang, Y.; Yang, W. A challenge for density functionals: Self-interaction error increases for systems with a noninteger number of electrons. *J. Chem. Phys.* **1998**, *109*, 2604–2608.
- (25) Ruzsinszky, A.; Perdew, J. P.; Csonka, G. I.; Vydrov, O. A.; Scuseria, G. E. Spurious fractional charge on dissociated atoms: Pervasive and resilient self-interaction error of common density functionals. *J. Chem. Phys.* **2006**, *125*, 194112.
- (26) Mori-Sánchez, P.; Cohen, A. J.; Yang, W. Many-electron self-interaction error in approximate density functionals. *J. Chem. Phys.* **2006**, *125*, 201102.
- (27) Anderson, P. W. Antiferromagnetism. Theory of superexchange interaction. *Phys. Rev.* **1950**, *79*, 350.
- (28) Kollmar, C.; Kahn, O. Ferromagnetic spin alignment in molecular systems: An orbital approach. *Acc. Chem. Res.* **1993**, *26*, 259–265.

- (29) Hart, J.; Rappé, A.; Gorun, S.; Upton, T. Ab initio calculation of the magnetic exchange interactions in (μ -oxo) diiron (III) systems using a broken symmetry wave function. *Inorg. Chem.* **1992**, *31*, 5254–5259.
- (30) Ernzerhof, M.; Perdew, J. P. Generalized gradient approximation to the angle- and system-averaged exchange hole. *J. Chem. Phys.* **1998**, *109*, 3313–3320.
- (31) Becke, A. D. Density-Functional thermochemistry. III. The Role of Exact Exchange. *J. Chem. Phys.* **1993**, *98*, 5648–5652.
- (32) Illas, F.; de PR Moreira, I.; Bofill, J.; Filatov, M. Extent and limitations of density-functional theory in describing magnetic systems. *Phys. Rev. B* **2004**, *70*, 132414.
- (33) Moreira, I. d. P.; Costa, R.; Filatov, M.; Illas, F. Restricted ensemble-referenced Kohn-Sham versus broken symmetry approaches in density functional theory: Magnetic coupling in Cu binuclear complexes. *J. Chem. Theory Comput.* **2007**, *3*, 764–774.
- (34) Peralta, J. E.; Melo, J. I. Magnetic exchange couplings with range-separated hybrid density functionals. *J. Chem. Theory Comput.* **2010**, *6*, 1894–1899.
- (35) Phillips, J. J.; Peralta, J. E. The role of range-separated Hartree-Fock exchange in the calculation of magnetic exchange couplings in transition metal complexes. *J. Chem. Phys.* **2011**, *134*, 034108.
- (36) Valero, R.; Costa, R.; de PR Moreira, I.; Truhlar, D. G.; Illas, F. Performance of the M06 family of exchange-correlation functionals for predicting magnetic coupling in organic and inorganic molecules. *J. Chem. Phys.* **2008**, *128*, 114103.
- (37) Costa, R.; Reta, D.; Moreira, I. d. P. R.; Illas, F. Post-B3LYP Functionals Do Not Improve the Description of Magnetic Coupling in Cu(II) Dinuclear Complexes. *J. Phys. Chem. A* **2018**, *122*, 3423–3432.

- (38) Lindgren, I. A statistical exchange approximation for localized electrons. *Int. J. Quantum Chem.* **1971**, *5*, 411–420.
- (39) Pederson, M. R.; Ruzsinszky, A.; Perdew, J. P. Communication: Self-interaction correction with unitary invariance in density functional theory. *J. Chem. Phys.* **2014**, *140*, 121103.
- (40) Yang, Z.-h.; Pederson, M. R.; Perdew, J. P. Full self-consistency in the Fermi-orbital self-interaction correction. *Phys. Rev. A* **2017**, *95*, 052505.
- (41) Pederson, M. R. Fermi orbital derivatives in self-interaction corrected density functional theory: Applications to closed shell atoms. *J. Chem. Phys.* **2015**, *142*, 064112.
- (42) Kao, D.-y.; Withanage, K.; Hahn, T.; Batool, J.; Kortus, J.; Jackson, K. Self-consistent self-interaction corrected density functional theory calculations for atoms using Fermi-Löwdin orbitals: Optimized Fermi-orbital descriptors for Li–Kr. *J. Chem. Phys.* **2017**, *147*, 164107.
- (43) Zope, R. R.; Baruah, T.; Jackson, K. A. FLOSIC 0.2. <https://flosic.org/>, based on the NRLMOL code of M. R. Pederson.
- (44) Yamamoto, Y.; Basurto, L.; Diaz, C. M.; Zope, R. R.; Baruah, T. FLOSIC software public release. https://github.com/FLOSIC/PublicRelease_2020/, based on the NRLMOL code of M. R. Pederson.
- (45) Diaz, C. M.; Basurto, L.; Adhikari, S.; Yamamoto, Y.; Ruzsinszky, A.; Baruah, T.; Zope, R. R. Self-interaction-corrected Kohn–Sham effective potentials using the density-consistent effective potential method. *J. Chem. Phys.* **2021**, *155*, 064109.
- (46) Diaz, C. M.; Baruah, T.; Zope, R. R. Fermi-Löwdin-orbital self-interaction correction using the optimized-effective-potential method within the Krieger-Li-Iafrate approximation. *Phys. Rev. A* **2021**, *103*, 042811.

- (47) Schwalbe, S.; Fiedler, L.; Kraus, J.; Kortus, J.; Trepte, K.; Lehtola, S. PyFLOSIC: Python-based Fermi–Löwdin orbital self-interaction correction. *J. Chem. Phys.* **2020**, *153*, 084104.
- (48) Aquino, F. W.; Shinde, R.; Wong, B. M. Fractional occupation numbers and self-interaction correction-scaling methods with the Fermi–Löwdin orbital self-interaction correction approach. *J. of Comput. Chem.* **2020**, *41*, 1200–1208.
- (49) Diaz, C. M.; Suryanarayana, P.; Xu, Q.; Baruah, T.; Pask, J. E.; Zope, R. R. Implementation of Perdew–Zunger self-interaction correction in real space using Fermi–Löwdin orbitals. *J. Chem. Phys.* **2021**, *154*, 084112.
- (50) Yamamoto, Y.; Romero, S.; Baruah, T.; Zope, R. R. Improvements in the orbitalwise scaling down of Perdew-Zunger self-interaction correction in many-electron regions. *J. Chem. Phys.* **2020**, *152*, 174112.
- (51) Withanage, K. P. K.; Akter, S.; Shahi, C.; Joshi, R. P.; Diaz, C.; Yamamoto, Y.; Zope, R.; Baruah, T.; Perdew, J. P.; Peralta, J. E. et al. Self-interaction-free electric dipole polarizabilities for atoms and their ions using the Fermi–Löwdin self-interaction correction. *Phys. Rev. A* **2019**, *100*, 012505.
- (52) Shahi, C.; Bhattarai, P.; Wagle, K.; Santra, B.; Schwalbe, S.; Hahn, T.; Kortus, J.; Jackson, K. A.; Peralta, J. E.; Trepte, K. et al. Stretched or noded orbital densities and self-interaction correction in density functional theory. *J. Chem. Phys.* **2019**, *150*, 174102.
- (53) Yamamoto, Y.; Diaz, C. M.; Basurto, L.; Jackson, K. A.; Baruah, T.; Zope, R. R. Fermi–Löwdin orbital self-interaction correction using the strongly constrained and appropriately normed meta-GGA functional. *J. Chem. Phys.* **2019**, *151*, 154105.
- (54) Sharkas, K.; Wagle, K.; Santra, B.; Akter, S.; Zope, R. R.; Baruah, T.; Jackson, K. A.;

- Perdew, J. P.; Peralta, J. E. Self-interaction error overbinds water clusters but cancels in structural energy differences. *Proc. Natl. Acad. Sci.* **2020**, *117*, 11283–11288.
- (55) Joshi, R. P.; Trepte, K.; Withanage, K. P.; Sharkas, K.; Yamamoto, Y.; Basurto, L.; Zope, R. R.; Baruah, T.; Jackson, K. A.; Peralta, J. E. Fermi-Löwdin orbital self-interaction correction to magnetic exchange couplings. *J. Chem. Phys.* **2018**, *149*, 164101.
- (56) Vargas, J.; Ufodu, P.; Baruah, T.; Yamamoto, Y.; Jackson, K. A.; Zope, R. R. Importance of self-interaction-error removal in density functional calculations on water cluster anions. *Phys. Chem. Chem. Phys.* **2020**, *22*, 3789–3799.
- (57) Jackson, K. A.; Peralta, J. E.; Joshi, R. P.; Withanage, K. P.; Trepte, K.; Sharkas, K.; Johnson, A. I. Towards efficient density functional theory calculations without self-interaction: The Fermi-Löwdin orbital self-interaction correction. *J. Phys. Conf. Ser.* **2019**, *1290*, 012002.
- (58) Johnson, A. I.; Withanage, K. P. K.; Sharkas, K.; Yamamoto, Y.; Baruah, T.; Zope, R. R.; Peralta, J. E.; Jackson, K. A. The effect of self-interaction error on electrostatic dipoles calculated using density functional theory. *J. Chem. Phys.* **2019**, *151*, 174106.
- (59) Trepte, K.; Schwalbe, S.; Hahn, T.; Kortus, J.; Kao, D.-Y.; Yamamoto, Y.; Baruah, T.; Zope, R. R.; Withanage, K. P. K.; Peralta, J. E. et al. Analytic atomic gradients in the Fermi-Löwdin orbital self-interaction correction. *J. Comput. Chem.* **2019**, *40*, 820–825.
- (60) Withanage, K. P. K.; Trepte, K.; Peralta, J. E.; Baruah, T.; Zope, R.; Jackson, K. A. On the Question of the Total Energy in the Fermi-Löwdin Orbital Self-Interaction Correction Method. *J. Chem. Theory Comput.* **2018**, *14*, 4122–4128.

- (61) Akter, S.; Yamamoto, Y.; Diaz, C. M.; Jackson, K. A.; Zope, R. R.; Baruah, T. Study of self-interaction errors in density functional predictions of dipole polarizabilities and ionization energies of water clusters using Perdew–Zunger and locally scaled self-interaction corrected methods. *J. Chem. Phys.* **2020**, *153*, 164304.
- (62) Sharkas, K.; Li, L.; Trepte, K.; Withanage, K. P. K.; Joshi, R. P.; Zope, R. R.; Baruah, T.; Johnson, J. K.; Jackson, K. A.; Peralta, J. E. Shrinking Self-Interaction Errors with the Fermi–Löwdin Orbital Self-Interaction-Corrected Density Functional Approximation. *J. Phys. Chem. A* **2018**, *122*, 9307–9315.
- (63) Pederson, M. R.; Baruah, T.; Kao, D.-y.; Basurto, L. Self-interaction corrections applied to Mg-porphyrin, C60, and pentacene molecules. *J. Chem. Phys.* **2016**, *144*, 164117.
- (64) Kao, D.-y.; Pederson, M.; Hahn, T.; Baruah, T.; Liebing, S.; Kortus, J. The Role of Self-Interaction Corrections, Vibrations, and Spin-Orbit in Determining the Ground Spin State in a Simple Heme. *Magnetochemistry* **2017**, *3*, 31.
- (65) Akter, S.; Yamamoto, Y.; Zope, R. R.; Baruah, T. Static dipole polarizabilities of polyacenes using self-interaction-corrected density functional approximations. *J. Chem. Phys.* **2021**, *154*, 114305.
- (66) Vydrov, O. A.; Scuseria, G. E.; Perdew, J. P.; Ruzsinszky, A.; Csonka, G. I. Scaling down the Perdew–Zunger self-interaction correction in many-electron regions. *J. Chem. Phys.* **2006**, *124*, 094108.
- (67) Perdew, J. P.; Ruzsinszky, A.; Sun, J.; Pederson, M. R. *Adv. At. Mol. Opt. Phys.*; Elsevier, 2015; Vol. 64; pp 1–14.
- (68) Bhattarai, P.; Wagle, K.; Shahi, C.; Yamamoto, Y.; Romero, S.; Santra, B.; Zope, R. R.; Peralta, J. E.; Jackson, K. A.; Perdew, J. P. A step in the direction

- of resolving the paradox of Perdew–Zunger self-interaction correction. II. Gauge consistency of the energy density at three levels of approximation. *J. Chem. Phys.* **2020**, *152*, 214109.
- (69) Zope, R. R.; Yamamoto, Y.; Diaz, C. M.; Baruah, T.; Peralta, J. E.; Jackson, K. A.; Santra, B.; Perdew, J. P. A step in the direction of resolving the paradox of Perdew–Zunger self-interaction correction. *J. Chem. Phys.* **2019**, *151*, 214108.
- (70) Bhattarai, P.; Santra, B.; Wagle, K.; Yamamoto, Y.; Zope, R. R.; Ruzsinszky, A.; Jackson, K. A.; Perdew, J. P. Exploring and enhancing the accuracy of interior-scaled Perdew–Zunger self-interaction correction. *J. Chem. Phys.* **2021**, *154*, 094105.
- (71) Akter, S.; Tellez, J. A. V.; Sharkas, K.; Peralta, J.; Jackson, K.; Baruah, T.; Zope, R. How well do self-interaction corrections repair the over-estimation of molecular polarizabilities in density functional calculations? *Phys. Chem. Chem. Phys.* **2021**,
- (72) Heisenberg, W. *Original Scientific Papers Wissenschaftliche Originalarbeiten*; Springer, 1985; pp 580–597.
- (73) Ruiz, E.; Cano, J.; Alvarez, S.; Alemany, P. Broken symmetry approach to calculation of exchange coupling constants for homobinuclear and heterobinuclear transition metal complexes. *J. Comp. Chem.* **1999**, *20*, 1391–1400.
- (74) Nishino, M.; Yamanaka, S.; Yoshioka, Y.; Yamaguchi, K. Theoretical approaches to direct exchange couplings between divalent chromium ions in naked dimers, tetramers, and clusters. *J. Phys. Chem. A* **1997**, *101*, 705–712.
- (75) Polo, V.; Gräfenstein, J.; Kraka, E.; Cremer, D. Long-range and short-range Coulomb correlation effects as simulated by Hartree–Fock, local density approximation, and generalized gradient approximation exchange functionals. *Theor. Chem. Acc.* **2003**, *109*, 22–35.

- (76) Polo, V.; Gräfenstein, J.; Kraka, E.; Cremer, D. Influence of the self-interaction error on the structure of the DFT exchange hole. *Chem. Phys. Lett.* **2002**, *352*, 469–478.
- (77) Polo, V.; Kraka, E.; Cremer, D. Electron correlation and the self-interaction error of density functional theory. *Mol. Phys.* **2002**, *100*, 1771–1790.
- (78) Polo, V.; Kraka, E.; Cremer, D. Some thoughts about the stability and reliability of commonly used exchange–correlation functionals—coverage of dynamic and nondynamic correlation effects. *Theor. Chem. Acc.* **2002**, *107*, 291–303.
- (79) Perdew, J. P.; Savin, A.; Burke, K. Escaping the symmetry dilemma through a pair-density interpretation of spin-density functional theory. *Phys. Rev. A* **1995**, *51*, 4531–4541.
- (80) Ruiz, E.; Cano, J.; Alvarez, S.; Polo, V. Reply to "Comment on 'About the calculation of exchange coupling constants using density-functional theory: The role of the self-interaction error'" [J. Chem. Phys. 123, 164110 (2005)]. *J. Chem. Phys.* **2006**, *124*, 107102.
- (81) Adamo, C.; Barone, V.; Bencini, A.; Broer, R.; Filatov, M.; Harrison, N. M.; Illas, F.; Malrieu, J. P.; de P. R. Moreira, I. Comment on "About the calculation of exchange coupling constants using density-functional theory: The role of the self-interaction error" [J. Chem. Phys. 123, 164110 (2005)]. *J. Chem. Phys.* **2006**, *124*, 107101.
- (82) Pederson, M. R.; Lin, C. C. Localized and canonical atomic orbitals in self-interaction corrected local density functional approximation. *J. Chem. Phys.* **1988**, *88*, 1807–1817.
- (83) Luken, W. L.; Beratan, D. N. Localized orbitals and the Fermi hole. *Theor. Chem. Acc.* **1982**, *61*, 265–281.
- (84) Löwdin, P.-O. On the non-orthogonality problem connected with the use of atomic

- wave functions in the theory of molecules and crystals. *J. Chem. Phys.* **1950**, *18*, 365–375.
- (85) Vydrov, O. A.; Scuseria, G. E. A simple method to selectively scale down the self-interaction correction. *J. Chem. Phys.* **2006**, *124*, 191101.
 - (86) Ruzsinszky, A.; Perdew, J. P.; Csonka, G. I.; Vydrov, O. A.; Scuseria, G. E. Density functionals that are one- and two- are not always many-electron self-interaction-free, as shown for H_2^+ , He_2^+ , LiH^+ , and Ne_2^+ . *J. Chem. Phys.* **2007**, *126*, 104102.
 - (87) Romero, S.; Yamamoto, Y.; Baruah, T.; Zope, R. R. Local self-interaction correction method with a simple scaling factor. *Phys. Chem. Chem. Phys.* **2021**, *23*, 2406–2418.
 - (88) Porezag, D.; Pederson, M. R. Optimization of Gaussian basis sets for density-functional calculations. *Phys. Rev. A* **1999**, *60*, 2840–2847.
 - (89) Pederson, M. R.; Jackson, K. A. Variational mesh for quantum-mechanical simulations. *Phys. Rev. B* **1990**, *41*, 7453–7461.
 - (90) Perdew, J. P.; Wang, Y. Accurate and simple analytic representation of the electron-gas correlation energy. *Phys. Rev. B* **1992**, *45*, 13244–13249.
 - (91) Perdew, J. P.; Burke, K.; Ernzerhof, M. Generalized gradient approximation made simple. *Phys. Rev. Lett.* **1996**, *77*, 3865.
 - (92) Perdew, J. P.; Burke, K.; Ernzerhof, M. Generalized Gradient Approximation Made Simple [Phys. Rev. Lett. 77, 3865 (1996)]. *Phys. Rev. Lett.* **1997**, *78*, 1396–1396.
 - (93) Sun, J.; Ruzsinszky, A.; Perdew, J. P. Strongly constrained and appropriately normed semilocal density functional. *Phys. Rev. Lett.* **2015**, *115*, 036402.
 - (94) Furness, J. W.; Kaplan, A. D.; Ning, J.; Perdew, J. P.; Sun, J. Accurate and numerically efficient r2SCAN meta-generalized gradient approximation. *J. Phys. Chem. Lett.* **2020**, *11*, 8208–8215.

- (95) Saito, T.; Nishihara, S.; Yamanaka, S.; Kitagawa, Y.; Kawakami, T.; Yamada, S.; Isobe, H.; Okumura, M.; Yamaguchi, K. Symmetry and broken symmetry in molecular orbital description of unstable molecules IV: Comparison between single-and multi-reference computational results for antiaromatic molecules. *Theor. Chem. Acc.* **2011**, *130*, 749–763.
- (96) Steenbock, T.; Tasche, J.; Lichtenstein, A. I.; Herrmann, C. A Green’s-Function Approach to Exchange Spin Coupling As a New Tool for Quantum Chemistry. *J. Chem. Theory Comput.* **2015**, *11*, 5651–5664.
- (97) Bencini, A.; Totti, F.; Daul, C. A.; Doclo, K.; Fantucci, P.; Barone, V. Density Functional Calculations of Magnetic Exchange Interactions in Polynuclear Transition Metal Complexes. *Inorg. Chem.* **1997**, *36*, 5022–5030.
- (98) Dolg, M.; Wedig, U.; Stoll, H.; Preuss, H. Energy-adjusted abinitio pseudopotentials for the first row transition elements. *J. Chem. Phys.* **1987**, *86*, 866–872.
- (99) Martin, J. M. L.; Sundermann, A. Correlation consistent valence basis sets for use with the Stuttgart-Dresden-Bonn relativistic effective core potentials: The atoms Ga–Kr and In–Xe. *J. Chem. Phys.* **2001**, *114*, 3408–3420.
- (100) Pritchard, B. P.; Altarawy, D.; Didier, B.; Gibsom, T. D.; Windus, T. L. A New Basis Set Exchange: An Open, Up-to-date Resource for the Molecular Sciences Community. *J. Chem. Inf. Model.* **2019**, *59*, 4814–4820.
- (101) Perdew, J. P.; Schmidt, K. Jacob’s ladder of density functional approximations for the exchange-correlation energy. *AIP Conference Proceedings* **2001**, *577*, 1–20.
- (102) Ruiz, E.; Rodríguez-Forteza, A.; Cano, J.; Alvarez, S.; Alemany, P. About the calculation of exchange coupling constants in polynuclear transition metal complexes. *J. Comp. Chem.* **2003**, *24*, 982–989.

- (103) Cramer, C. J.; Smith, B. A. Trimethylenemethane. Comparison of multiconfiguration self-consistent field and density functional methods for a non-Kekulé hydrocarbon. *J. Phys. Chem.* **1996**, *100*, 9664–9670.
- (104) Rodriguez, E.; Reguero, M.; Caballol, R. The controversial ground state of tetramethyleneethane. An ab initio CI study. *J. Phys. Chem. A* **2000**, *104*, 6253–6258.
- (105) Zhang, J.; Zhang, H.; Wang, L.; Wang, R.; Wang, L. Effect of configuration and conformation on the spin multiplicity in xylylene type biradicals. *Sci. China, Ser. B: Chem.* **2000**, *43*, 524–530.
- (106) Reta Mañeru, D.; Pal, A. K.; Moreira, I. d. P.; Datta, S. N.; Illas, F. The Triplet–Singlet Gap in the m-Xylylene Radical: A Not So Simple One. *J. Chem. Theory Comput.* **2014**, *10*, 335–345.
- (107) Willett, R. D.; Gatteschi, D.; Kahn, O. *Magneto-structural correlations in exchange coupled systems*; D. Reidel: Dordrecht, 1985.
- (108) Bencini, A.; Gatteschi, D.; Zanchini, C. Anisotropic exchange in transition-metal dinuclear complexes. 6. Bis(–.mu.–chloro)bis(dichlorocuprates(II)). *Inorg. Chem.* **1985**, *24*, 704–708.
- (109) Calzado, C. J.; Cabrero, J.; Malrieu, J. P.; Caballol, R. Analysis of the magnetic coupling in binuclear complexes. I. Physics of the coupling. *J. Chem. Phys.* **2002**, *116*, 2728–2747.
- (110) Islam, M. F.; Nossa, J. F.; Canali, C. M.; Pederson, M. First-principles study of spin-electric coupling in a Cu₃ single molecular magnet. *Phys. Rev. B* **2010**, *82*, 155446.
- (111) Pederson, M. R.; Khanna, S. N. Electronic structure and magnetism of Mn₁₂O₁₂ clusters. *Phys. Rev. B* **1999**, *59*, R693–R696.

- (112) Miralles, J.; Daudey, J.-P.; Caballol, R. Variational calculation of small energy differences. The singlet-triplet gap in $[\text{Cu}_2\text{Cl}_6]^{2-}$. *Chem. Phys. Lett.* **1992**, *198*, 555–562.
- (113) Castell, O.; Miralles, J.; Caballol, R. Structural dependence of the singlet-triplet gap in doubly bridged copper dimers: A variational CI calculation. *Chem. Phys.* **1994**, *179*, 377–384.